

Thermal Isomerizations of *cis,anti,cis*-Tricyclo[7.4.0.0^{2,8}]tridec-10-ene

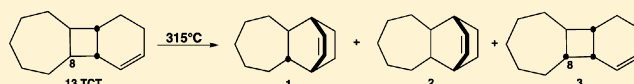
Phyllis A. Leber,^{*,†} George R. Mann, III,[†] William Hancock-Cerutti,[†] Matthew F. Wiperman,[†] Sylvia Zohrabian,[†] Ryan M. Bell,[†] and John E. Baldwin[‡]

[†]Department of Chemistry, Franklin and Marshall College, Lancaster, Pennsylvania 17604, United States

[‡]Department of Chemistry, Syracuse University, Syracuse, New York 13244, United States

Supporting Information

ABSTRACT: *cis,anti,cis*-Tricyclo[7.4.0.0^{2,8}]tridec-10-ene (**13TCT**) undergoes [1,3] sigmatropic rearrangements at 315 °C in the gas phase to the *si* product **1** and to the *sr* product **2** with *si*/*sr* = 2.1. The dominant thermal isomerization process, however, is epimerization at C8 to afford product **3**. That stereomutation at C8 occurs 50% faster than the *si* and *sr* shifts combined.



INTRODUCTION

The theory-based paradigm for thermal sigmatropic reactions enunciated by Woodward and Hoffmann in *The Conservation of Orbital Symmetry* provided clear guidance for mechanistic and stereochemical expectations.¹ For [1,3] carbon shifts such as vinylcyclobutane-to-cyclohexene isomerizations, they would, according to the rubric, take place with symmetry-allowed *si* (suprafacial, inversion) and *ar* (antarafacial, retention) stereochemical outcomes, if formed through concerted paths, and not give symmetry-forbidden *sr* (suprafacial, retention) and *ai* (antarafacial, inversion) products unless nonconcerted reactions were involved.

Thermal isomerizations of chiral *trans*-1,2-divinyl- and *trans*-1,2-*trans,trans*-dipropenylcyclobutanes were studied by Berson and Dervan in 1973. All four possible stereochemical outcomes as these two monocyclic vinylcyclobutanes formed isomeric cyclohexenes were evident in product mixtures.² The suprafacial paths from vinylcyclobutanes to cyclohexenes were largely preferred, and *si*/*sr* ratios were slightly greater than 1. Antarafacial stereochemical paths were relatively minor, but they were detected. Given the geometric constraints inherent in most bicyclic vinylcyclobutanes, [1,3] carbon shift reactions cannot give antarafacial products. Only symmetry-allowed *si* and symmetry-forbidden *sr* products might be formed, at different rates. Experimentally determined *si*/*sr* ratios would afford stereochemical and mechanistic distinctions between concerted and diradical-mediated routes for [1,3] shifts of bicyclic vinylcyclobutanes. The *si*/*sr* ratio for such isomerizations has become a default standard for assessing the degree of concert for these sigmatropic reactions.

Thermal reactions of bicyclo[3.2.0]hept-2-enes³ and bicyclo[4.2.0]oct-2-enes⁴ revealed some stark differences with respect to product stereoselectivity and preferred exit channels. The *si*/*sr* ratios are larger for bicyclo[3.2.0]hept-2-enes³ than for bicyclo[4.2.0]oct-2-enes,⁴ systems of greater conformational flexibility. Compared to the strong preference for *si* [1,3] shifts favored by bicyclo[3.2.0]hept-2-enes, bicyclo[4.2.0]oct-2-enes exhibit dramatically different thermal behavior. The dominant

rearrangement mode for 8-*exo*-substituted bicyclo[4.2.0]oct-2-enes at 275 °C leads to a one-centered stereomutation, an epimerization, at C8. The next most prominent thermal process is fragmentation. The [1,3] carbon migrations, only marginally stereoselective, are least important.

In order to examine the effect of conformational mobility at the migrating carbon on [1,3] shifts, we have studied a series of three tricyclic vinylcyclobutanes, labeled by the acronyms **11TCU**, **12TCD**, and **13TCT**, combining the number of carbons involved, the common tricyclic designation (TC), and the initial for the olefinic name. Each of the three contains a bicyclo[4.2.0]oct-2-ene core; they differ only in the ring size in which the migrating carbon resides: the tricyclics contain five-, six-, and seven-membered rings fused with the bicyclo[4.2.0]oct-2-ene substructure in **11TCU**, **12TCD**, and **13TCT**, respectively (Table 1).

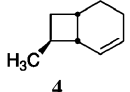
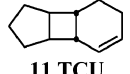
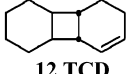
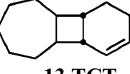
The value in studying tricyclic vinylcyclobutanes is 3-fold. First, epimerization at the carbon involved in [1,3] shifts might well be assumed to be geometrically prohibited; the *si* and *sr* sigmatropic shifts could then afford the sole isomerization exit channels. Second, the tricyclics would serve as a test of the empirical phenomenon of product stability control observed for the *si* and *sr* stereoisomeric products derived from bicyclic vinylcyclobutanes.³ This prediction was predicated on the assumption that a *trans*-ring juncture in the resultant tricyclic *si* product would reduce its thermodynamic stability relative to the tricyclic *sr* product. Third, the conformational restrictions on the migrating carbon in each tricyclic reactant would serve to assess rotational propensities reflected by stereochemical outcomes in [1,3] carbon shift products. In a previous paper we had argued that the “*si*/*sr* ratio is an extremely sensitive probe of the rotational propensity of the migrating carbon and, as a corollary, the lifetime of the resultant biradical intermediate.”^{4d}

The first premise was proven true for both **11TCU** and **12TCD**, neither of which experienced one-centered stereo-

Received: February 6, 2012

Published: March 15, 2012

Table 1. Stereochemistry of [1,3] Shifts for **4** and Tricyclic Vinylcyclobutanes

Compound	temp(°C)	si (%)	sr (%)	si/sr	Ref.
 4	275-315	71	29	2.4	4a
 11 TCU	315	0	100	0	5a
 12 TCD	315	71	29	2.4	5b
 13 TCT	315	68	32	2.1	this work

mutations at the carbon involved in one or two sigmatropic shifts. We were intrigued as to whether or not this trend would also persist for **13TCT**. As shown in Table 1, **11TCU** is restricted to a symmetry-forbidden *sr* migration^{5a} whereas **12TCD** undergoes a [1,3] shift with *si/sr* = 2.4,^{5b} a value identical to that observed for the analogous bicyclic vinylcyclobutane 8-*exo*-methylbicyclo[4.2.0]oct-2-ene (**4**). The different stereoselectivities exhibited by **11TCU** and **12TCD** are inconsistent with product stability control because the less thermodynamically stable *si* product is modestly favored once it can be accessed via an exothermic process (Table 2). The

Table 2. Thermochemical Analysis (ΔH_{rxn} in kcal/mol) of Tricyclics

Compound	si	sr	ep	ref.
11TCU	+12.2	-10.7	+19.7 ^a	5a
12TCD	-2.9	-9.4	+9.7 ^a	5b
13TCT	-10.7	-9.3	+4.0	this work ^a

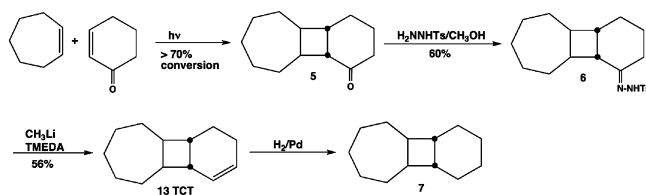
^aGaussian B3LYP/6-31G** energy calculations for ground state optimized structures.

stereochemical outcomes for **11TCU** and **12TCD** might well reflect a difference in rotational propensities displayed by migrating carbons. We have therefore sought to examine the thermal behavior of **13TCT** to assess the importance of dynamic effects on the migrating carbon C8.

The primary conclusion afforded by the thermal study of **12TCD** is that product-determining events are closely linked to the nature of the diradical intermediate.^{5b} The alkyl, allyl diradical intermediate structure proposed for **12TCD** therefore would serve as a useful predictive model for the thermal reactions of **13TCT**. Fundamentally, the diradical intermediate derived from **12TCD** consists of two separate components, a cyclohexyl radical⁶ subunit and a cyclohexenyl radical⁷ subunit, connected by a covalent bond.^{5b} The planarity at all three carbons in the allyl moiety of the cyclohexenyl radical and the fixed facial relationship of the cyclohexyl radical relative to this planar moiety impose limits on accessible product exit channels. The point of difference between **12TCD** and **13TCT** is clear; the latter, as a function of a cycloheptyl substitution in **13TCT** for a cyclohexyl in **12TCD**, would afford diradical transition structures consisting of cycloheptyl and cyclohexenyl radical subunits. Fortunately, abundant structural comparisons of cyclohexyl and cycloheptyl radicals already exist in the literature.⁸

RESULTS AND DISCUSSION

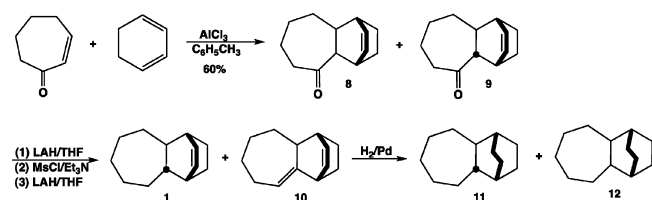
Syntheses and Structural Characterizations. Compound **13TCT** was successfully prepared using a synthetic sequence analogous to that affording **12TCD**,^{5b} the structure of which was unambiguously confirmed by its conversion to the known compound *cis,anti,cis*-tricyclo[6.4.0.0^{2,7}]dodecane⁹ upon catalytic hydrogenation; that is, the carbon skeleton and stereochemistry of **13TCT** can be established by the application of a proven route for the synthesis of **12TCD** to that of **13TCT**. Thus, the ketone precursor of **13TCT** was readily accessible by photochemical cycloaddition of cycloheptene and 2-cyclohexenone using a 450-W medium-pressure mercury lamp (Scheme 1). The reaction reached 70%

Scheme 1. Synthesis of *cis,anti,cis*-Tricyclo[7.4.0.0^{2,8}]tridec-10-ene (**13TCT**)

conversion after ca. 30 h of irradiation. Characterization of the ketone cycloadduct **5** by ¹³C NMR was achieved using a column chromatography fraction of greater than 70% purity: δ 215.0 (C=O), 47.8 (CH), 42.1 (CH), 41.7 (CH), 40.3 (CH₂), 38.0 (CH), 32.8 (CH₂), 32.2 (CH₂), 32.0 (CH₂), 29.3 (CH₂), 29.2 (CH₂), 27.0 (CH₂), 21.2 (CH₂). Mass spectral analysis afforded a molecular ion peak at *m/z* 192, a base peak at *m/z* 97, and an M+1:M ratio of 14.3% consistent with a compound containing 13 carbons.

Tosylhydrazide formation from the partially purified tricyclic ketone resulted in a colorless crystalline solid **6** with a narrow melting range (153–154 °C); the IR spectrum of **6** showed a distinctive N–H stretch at 3217 cm⁻¹. The Shapiro modification of the Bamford–Stevens reaction, which was previously employed for the preparation of **12TCD**,^{5b} gave **13TCT** (¹³C NMR: δ 131.0 (=CH), 126.0 (=CH), 46.7 (CH), 38.8 (CH), 36.0 (CH), 35.5 (CH), 32.7 (CH₂), 32.5 (CH₂), 32.4 (CH₂), 30.1 (CH₂), 29.0 (CH₂), 23.6 (CH₂), 21.6 (CH₂)). A molecular ion peak at *m/z* 176 and HRMS confirmed the molecular formula of **13TCT** as C₁₃H₂₀. Catalytic reduction of **13TCT** yielded *cis,anti,cis*-tricyclo[7.4.0.0^{2,8}]tridecane **7** with only seven nonequivalent carbons due to the plane of symmetry in the molecule: δ 42.1 (2CH), 36.2 (2CH), 32.7 (CH₂), 32.1 (2CH₂), 29.5 (2CH₂), 28.0 (2CH₂), 23.0 (2CH₂).

The carbon framework of product **1** was accessed by Diels–Alder cycloaddition of 1,3-cyclohexadiene and 2-cycloheptenone using an aluminum trichloride catalyst (Scheme 2).¹⁰ Spectral data of ketones **8** and **9** matched the literature values.¹⁰ Subjecting the ketone mixture to the reduction methodology^{5b} that worked well for the preparation of *cis,endo*-tricyclo[6.2.2.0^{2,7}]dodec-9-ene gave compound **1** and *endo*-tricyclo[7.2.2.0^{2,8}]trideca-2,10-diene **10** in a 1:4 ratio. The ¹³C NMR spectrum of **1** showed 13 nonequivalent carbons: δ 136.1 (=CH), 131.6 (=CH), 44.0 (CH), 43.3 (CH), 36.7 (CH), 36.4 (CH), 34.5 (CH₂), 30.3 (CH₂), 29.3 (CH₂), 28.5 (CH₂), 28.1 (CH₂), 24.9 (CH₂), 18.0 (CH₂), values quite analogous to those reported for *trans*-tricyclo[6.2.2.0^{2,7}]dodec-9-ene.^{5b}

Scheme 2. Synthesis of *trans*-Tricyclo[7.2.2.0^{2,8}]tridec-10-ene (1)

Isomer 2, which would have only seven nonequivalent carbons due to the plane of symmetry bisecting the molecule, was not found in the reaction mixture obtained by the reductions of ketones 8 and 9. The anticipated ¹³C NMR evidence for 2 was secured from a preparative thermal reaction of 13TCT: δ 133.1 (=CH), 46.4 (CH), 38.9 (CH), 34.0 (CH₂), 32.5 (CH₂), 25.6 (CH₂), 19.4 (CH₂), values quite comparable to the corresponding chemical shifts for the *sr* product obtained from 12TCD.^{5b} The mass spectrum of 2 also acquired from the thermal reaction mixture is consistent with a hydrocarbon of molecular formula C₁₃H₂₀ and shows a weak molecular ion peak at *m/z* 176 and a base peak of 80, corresponding to a stable cyclohexadienyl radical cation.

The structure of the major E₂ side product 10 (Scheme 2) was deduced from its synthetic precursor and its ¹³C NMR spectral data: δ 149.1 (=C), 132.5 (=CH), 132.3 (=CH), 120.3 (=CH), 47.2 (CH), 41.9 (CH), 39.3 (CH), 34.4 (CH₂), 32.5 (CH₂), 28.9 (CH₂), 27.5 (CH₂), 26.1 (CH₂), 25.4 (CH₂). Mass spectral analysis of 1 gave a molecular ion peak at *m/z* 176 and a base peak at *m/z* 80; relevant mass spectral data for 10 are a molecular ion peak at *m/z* 174 and a base peak at *m/z* 146 due to loss of ethylene.

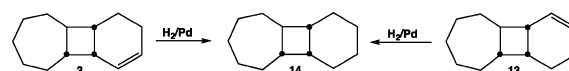
Catalytic hydrogenation of a mixture of 1 and 10 resulted in a 7:3 ratio of 11:12. The ¹³C NMR spectral data for 11 and 12 respectively are as follows: δ 42.4 (2CH), 33.3 (2CH₂), 31.4 (2CH), 30.7 (CH₂), 28.9 (2CH₂), 27.5 (2CH₂), 21.0 (2CH₂); δ 42.2 (2CH), 32.2 (2CH), 32.0 (2CH₂), 31.3 (CH₂), 27.1 (2CH₂), 25.4 (2CH₂), 20.8 (2CH₂). Independent structural verification of thermal product 2 was achieved by catalytic hydrogenation of the thermal reaction mixture to give, by GC analysis,¹¹ an 11:12 ratio of 2.2, a value virtually identical to the *si/sr* (1:2) ratio of 2.1(5) (Table 1).

The major thermal product 3 was identified as the C8 epimer of 13TCT. Because most fractions of ketone 5 contained 30–40% of a mixture of minor stereoisomers of 5, running the Shapiro reaction on a series of successive crops of impure tosylhydrazone derivatives yielded first the stereoisomeric hydrocarbon 13 (δ 129.8 (=CH), 127.8 (=CH), 48.2 (CH), 41.8 (CH), 38.6 (CH), 33.7 (CH), 33.6 (CH₂), 30.0 (CH₂), 29.0 (CH₂), 26.2 (CH₂), 26.1 (CH₂), 23.2 (CH₂), 22.3 (CH₂) and then product 3 (δ 128.4 (=CH), 127.7 (=CH), 45.4 (CH), 40.4 (CH), 37.6 (CH), 33.6 (CH), 32.9 (CH₂), 29.8 (CH₂), 29.2 (CH₂), 27.6 (CH₂), 25.9 (CH₂), 21.7 (CH₂), 21.3 (CH₂)). Gaussian ¹³C NMR simulations, providing only estimated chemical shift values, proved diagnostic in differentiating between compounds 3 and 13, two stereoisomers of 13TCT, based on the chemical shift difference between the two sp²-hybridized carbons (Table 3).

The definitive structure proof of 3 (Scheme 3) was based on the observation that both 3 and 13, upon catalytic hydrogenation, are converted to the same saturated hydrocarbon 14 with a distinctive ¹³C NMR spectrum of 13 peaks: δ 42.7 (CH), 40.7 (CH), 37.7 (CH), 34.0 (CH), 33.9 (CH₂), 30.3 (CH₂),

Table 3. Experimental and Simulated ¹³C NMR Chemical Shifts

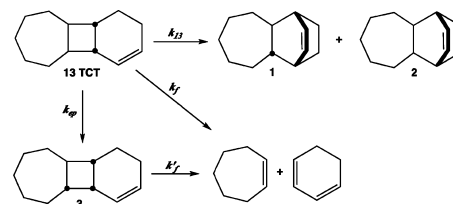
Compound	δ (C _{sp²})	δ (C _{sp³})	Exptl Diff. (ppm)	Sim. Diff. (ppm)
13TCT	131.0	126.0	5.0	5
3	128.4	127.7	0.7	0.5
13	129.8	127.8	2.0	3

Scheme 3. Catalytic Hydrogenation of Two 13TCT Stereoisomers (3 and 13) To Yield *trans,cis*-Tricyclo[7.4.0.0^{2,8}]tridecane (14)

29.3 (CH₂), 26.6 (CH₂), 26.2 (CH₂), 25.5 (CH₂), 24.2 (CH₂), 23.8 (CH₂), 22.9 (CH₂). The *trans,cis*-stereochemistry of 14 was confirmed by comparison of its ¹³C NMR chemical shifts with the corresponding signals for *trans,cis*-tricyclo[6.4.0.0^{2,7}]-dodecane.⁹

Kinetic Analysis. The thermal reactions of 13TCT, as shown in Scheme 4, were followed at 315 °C in sealed base-

Scheme 4. Kinetic Profile and Thermal Reactions of 13TCT



treated capillary tubes that had been subjected to three freeze–pump–thaw cycles prior to closure. Capillary GC analysis provided relative concentration versus reaction time data for 13TCT as well as products 1, 2, and 3; all components were well-resolved and eluted in the following order: 1, 2, 13TCT, 3 (Figure 1). The relative elution order for 1 and 2 is consistent with that previously reported for the *si* and *sr* products of 12TCD. The value of the rate constant for overall loss of 13TCT, $k_0 = 1.31 \times 10^{-5} \text{ s}^{-1}$, and its component rate constants were obtained using the Solver function in Microsoft Excel to fit experimental concentrations to the first-order exponential

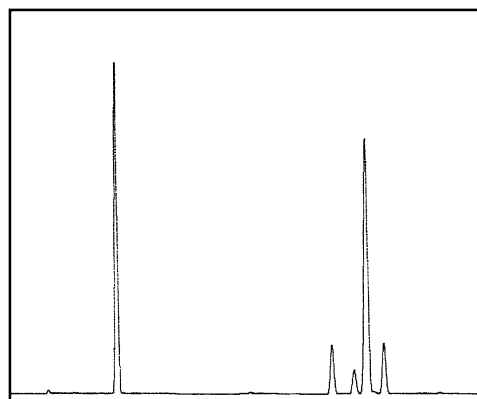


Figure 1. Capillary GC analysis¹¹ of gas-phase thermal reaction mixture after 737.5 min (12.3 h) at 315 °C: tetradecane (internal standard), 1, 2, 13TCT, and 3 (from left to right).

rate expressions based on the kinetic profile shown in Scheme 4. All other rate constants determined accordingly are as follows: $k_{si} = 2.8 \times 10^{-6} \text{ s}^{-1}$, $k_{sr} = 1.3 \times 10^{-6} \text{ s}^{-1}$, $k_{ep} = 6.1 \times 10^{-6} \text{ s}^{-1}$, and $k_f = 3.3 \times 10^{-5} \text{ s}^{-1}$. The *si*/*sr* value thus derived from k_{si} and k_{sr} is 2.15, and $k_{13} = k_{si} + k_{sr} = 4.1 \times 10^{-6} \text{ s}^{-1}$. The rate of direct fragmentation k_f was determined as $2.2 \times 10^{-6} \text{ s}^{-1}$ by curve fitting. The difference between k_o and the sum ($k_{si} + k_{sr} + k_{ep}$) approximated k_f as $2.9 \times 10^{-6} \text{ s}^{-1}$. The relative order of importance of all kinetic processes is $k_{ep} > k_{13} > k_f$ (Table 4).

Table 4. Exit Channels for 4 and Tricyclic Vinylcyclobutane Analogs

Compound	temp (°C)	% [1,3]	% epim	% frag	k_{13}/k_f	k_{ep}/k_{13}	Relative Rates
4	275	15	47	38	0.4	3.1	$k_{ep} > k_f > k_{13}$
11TCU	315	32	0	68	0.5	0	$k_f > k_{13}$
12TCD	315	54	0	42	1.3	0	$k_{13} > k_f$
13TCT	315	33	49	18	1.9	1.5	$k_{ep} > k_{13} > k_f$

The kinetic results for 13TCT yield an *si*/*sr* ratio of 2.1 (Table 1), a value comparable to that for 12TCD. The thermal profile of 13TCT however is quite distinct compared to the tricyclic vinylcyclobutanes 11TCU and 12TCD in that the major thermal isomerization process is epimerization at C8, not [1,3] sigmatropic rearrangements. While 13TCT mimics the bicyclo[4.2.0]oct-2-enes in this regard, fragmentation is only a minor thermal pathway for 13TCT in contrast to the product distribution observed for 4 (Table 4).

Neither 11TCU nor 12TCD undergoes a stereomutation at a $-\text{CH}-$ moiety able to achieve one or two [1,3] shifts. The relative contribution of the [1,3] rearrangements and fragmentation processes in each, however, varies as a function of the extent of rotational torque accessible to the respective migrating carbon. Since [1,3] shifts can compete more effectively with fragmentation when a greater range of dynamic motion is available, the k_{13}/k_f ratio of 0.5 for 11TCU more than doubles to 1.3 for 12TCD (Table 4). In 13TCT, [1,3] migration is favored over fragmentation by a factor of ca. 2 ($k_{13}/k_f = 1.9$). The most dramatic difference in comparing 13TCT with 12TCD and 11TCU, however, is that epimerization at C8 is the dominant thermal isomerization for 13TCT: $k_{ep}/k_{13} = 1.5$, while for 11TCU and 12TCD it is 0. For bicyclic system 4 it is 3.1 (Table 4).

The lack of any significant retro-Diels–Alder fragmentation of 1 and 2 to cycloheptene and 1,3-cyclohexadiene under the reaction conditions has been surmised from both prior experimental work^{4,5} and the relative invariance of the *si*/*sr* ratio. The similarity in the *si*/*sr* ratios for 4 and both 12TCD and 13TCT in Table 1 is probably not coincidental but rather an experimental measure of the inherent rotational propensities of the migrating carbon in these [4.2.0] olefins where a migrating carbon carries an *exo*-alkyl substituent. The respective migrating carbons in 4 and in both 12TCD and 13TCT possess comparable rotational abilities, suggesting that a rotational contribution only manifests itself once the bond between the migrating carbon and the migration origin has completely broken and the diradical intermediate has fully formed.

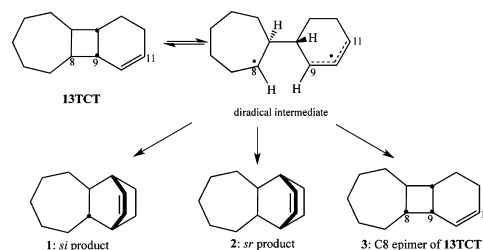
Conformational flexibility at the migrating carbon thus exerts a minimal impact on the *si*/*sr* ratio as soon as there is sufficient rotational torque for a dynamic partitioning between the *si* and

sr options. Northrop and Houk¹² have computationally estimated that the *si* and *sr* transition structures for the vinylcyclobutane-to-cyclohexene conversions differ by 1.0 kcal/mol, a difference in activation energy that equates with an *si*/*sr* value of 2.35. Both 12TCD and 13TCT converge well toward this value.

The predominant epimerization product 3 is consistent with a diradical intermediate, and the large preference for isomerization pathways (49% epimerization +33% [1,3] migrations) rather than fragmentation is a measure of the inherent inward rotational trajectory^{12–14} of C8 whether the isomerization product is 1 or 2 or 3. Significantly, direct fragmentation is reduced to a minor pathway as the conformational flexibility of the ring containing the migrating carbon increases in the tricyclic series shown in Table 4. The pentamethylene tether in 13TCT allows for the greatest possible range of motion for the cycloalkyl radical subunit and thus gives rise to contrasting product outcomes for tricyclics 12TCD and 13TCT.

We have previously argued that the 12TCD product ratios are consistent with the dynamic conformational space accessible to the resultant cyclohexyl, cyclohexenyl diradical intermediate.^{5b} The corresponding diradical transition structure formed from 13TCT would be a cycloheptyl, cyclohexenyl diradical intermediate. It is noteworthy that cyclohexyl and cycloheptyl radicals differ in their rate of ring inversion. The greater ease of cycloheptyl radical ring inversion can be attributed to more degrees of freedom afforded by the greater “number of rotatable C–C bonds.”^{8b} The enhanced conformational flexibility of the cycloheptyl radical might well permit the radical center at the migrating carbon to invert while the migrating carbon is still in close proximity to the migration origin on the cyclohexenyl radical subunit, thus enabling the process of epimerization forming product 3 to compete effectively with the [1,3] exit channels yielding products 1 and 2. Homolytic cleavage of the C8–C9 bond in 13TCT results in a cycloheptyl, cyclohexenyl diradical with sufficient flexibility to access exit channels to products 1, 2, and 3 (Scheme 5).

Scheme 5. Mechanistic Analysis of 13TCT Thermal Chemistry



The most unexpected observation in this study is that product 3 does not undergo subsequent reversion to 13TCT, a reaction estimated to be exothermic by 4 kcal/mol (Table 2), but instead fragments to cycloheptene and 1,3-cyclohexadiene.¹⁵ Dreiding models of 3 show that the trans ring juncture between the seven-membered and cyclobutane rings imparts significant rigidity to the folded cyclobutane moiety such that the migrating carbon C8 in 3 experiences negligible conformational flexibility compared to stereoisomer 13TCT. A computer-generated model (Figure 2) of 3 shows C8 in the puckered cyclobutane conformation is pointed away from the cyclohexene ring, which poses an obvious geometric constraint

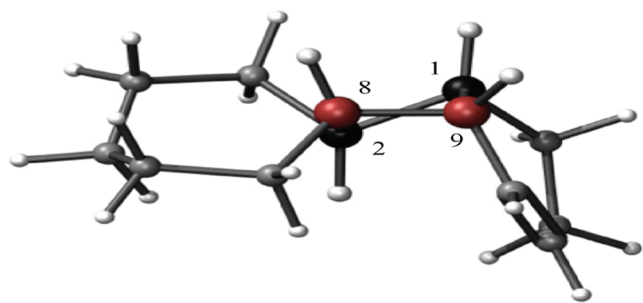


Figure 2. Computer-generated model of compound 3.

to an inward rotational trajectory. This factor may thus predispose **3** toward fragmentation rather than epimerization to **13TCT**: as the C8–C9 bond ruptures and gains access to a diradical transition region, it may extend the C8–C2–C1–C9 torsional angle so as to distance C8 further from C9 and effect rotation about H–C2–C8–H leading toward forming the fragmentation product *cis*-cycloheptene.

CONCLUSIONS

The simplest mechanistic explanation for the thermal behavior of **13TCT** here postulated depends on homolytic cleavage of the C8–C9 bond to generate a cycloheptyl, cyclohexenyl diradical intermediate that can partition itself between isomerization products **1**, **2**, and **3** and fragmentation products cycloheptene and 1,3-cyclohexadiene. It undergoes [1,3] carbon sigmatropic rearrangements to both symmetry-allowed *si* (**1**) and symmetry-forbidden *sr* (**2**) products reflecting an *si/sr* = 2.1 ratio. In this regard, its competitive thermal sigmatropic shift paths differ little from the *si/sr* = 2.4 ratio balance recorded for the **12TCD** tricyclic.

Our study of tricyclic vinylcyclobutanes initially anticipated that conformational restrictions on a migrating carbon residing in the third ring of what was fundamentally a bicyclo[4.2.0]oct-2-ene reactive moiety would preclude an epimerization (formally a [1,1] rearrangement), violate product stability control, and restrict torsional rotations. A modeling study¹⁶ of **11TCU** confirmed that the rigid cyclopentyl radical subunit in the diradical transition structure produced by **11TCU** did indeed prohibit rotation, for neither an *si* [1,3] carbon shift nor an epimerization at C8 was observed. As seen in Table 1, conversion of **12TCD** to an *si* product was realized, but it could not achieve an epimerization. As Table 2 rationalizes, an epimerization of **12TCD** would have been decisively impeded by a 10 kcal/mol endothermodynamic restraint. The current study of **13TCT** has shown that a seven-membered ring can energetically accommodate *si* and *sr* [1,3] shifts as well as the epimerization giving compound **3**, the C8 epimer of **13TCT**. The process of epimerization itself offers compelling evidence for a diradical transition structure.

Regarding product stability control, **13TCT** is the only one of the tricyclic reactants studied where the *si* [1,3] rearrangement product is more thermodynamically stable than the *sr* product. Calculated estimated ΔH_{rxn} values for isomerizations labeled for *si*, *sr*, and *ep* products in Table 2 show that the three *sr* products with *cis* ring junctures vary little in relative stability whereas the energy range for *si* products with *trans* ring junctures spans a 23 kcal/mol gap between the **11TCU** and **13TCT** tricyclic reactants. Compounds **1** and **3** both possess *trans* ring junctures yet are energetically accessible isomerization products for **13TCT**.

Dynamic factors appear to exert a strong effect on the exit channels available to **13TCT**. When the migrating carbon is embedded in a seven-membered ring, as it is in **13TCT**, its enhanced mobility as the diradical is formed allows the molecule to access a greater range of conformational space. Apparently there is sufficient conformational flexibility at C8 once the diradical transition region is reached that epimerization, the dominant thermal pathway for bicyclo[4.2.0]oct-2-enes such as **4**, is quite facile for **13TCT** in spite of its tethered structural limitations, for epimerization effectively competes with [1,3] sigmatropic rearrangements. This result is intriguing because epimerization occurs though it reverses the motion dictated by conservation of angular momentum.¹³

Thermal reactions of tricyclic vinylcyclobutanes, taken in their entirety, are governed by dynamic opportunities that a diradical transition structure, depending on its conformational flexibility, can exploit. The nature of the exit channels and the associated product distributions can be accounted for by the relative degree of rotational fluidity inherent in the transition structure without recourse to stereochemical factors related to conservation of orbital symmetry. Other work underway in our laboratory may well reinforce the finding that diradical transition structures derived from bicyclo[4.2.0]oct-2-enes and selected tricyclic analogs have a substantially greater ability to explore conformational space than diradicals generated from bicyclo[3.2.0]hept-2-enes.

EXPERIMENTAL SECTION

cis,anti,cis-Tricyclo[7.4.0.0^{2,8}]tridecan-10-one (5). A mixture of 25 mL of cycloheptene (Aldrich, 97%) and 5 mL (5.0 g, 5.2 mmol) of 2-cyclohexen-1-one was combined in a photochemical reactor immersion well cooled with ice and fitted with a thermometer and condenser. The reaction mixture was irradiated for a total of ca. 30 h with a 450-W Hanovia medium pressure mercury lamp placed inside a Pyrex sleeve. Reaction progress was monitored via analytical GC by determining the decrease in the amount of 2-cyclohexenone over time. Concentration of the reaction mixture under reduced pressure afforded a mixture of monoketone and diketone dimers. A 6.0 g sample of the photochemical product mixture was partially purified by flash column chromatography (SiO₂, 9:1 pentane/ether), affording 1.5 g of a colorless liquid obtained by combining and concentrating the column fractions corresponding to greater than 70% of the most abundant ketone **5**. ¹H NMR (500 MHz, CDCl₃) δ 2.49 (m, 2H), 2.41 (m, 2H), 2.19 (m, 2H), 1.94 (m, 1H), 1.81 (m, 4H), 1.73 (m, 2H), 1.57 (m, 4H), 1.45 (m, 1H), 1.23 (m, 1H), 1.07 (m, 1H). ¹³C NMR (125 MHz, CDCl₃) δ 215.0 (C=O), 47.8 (CH), 42.1 (CH), 41.7 (CH), 40.3 (CH₂), 38.0 (CH), 32.8 (CH₂), 32.2 (CH₂), 32.0 (CH₂), 29.3 (CH₂), 29.2 (CH₂), 27.0 (CH₂), 21.2 (CH₂). FTIR (neat) ν_{max} 2916, 2848, 1697, 1450 cm⁻¹. LRMS (EI) *m/z* 192 (M⁺, 56), 163 (41), 97 (100), 81 (51), 67 (41).

cis,anti,cis-Tricyclo[7.4.0.0^{2,8}]tridecan-10-one tosylhydrazone (6). To a solution of toluenesulfonylhydrazide (2.6 g, 14 mmol) in 50 mL of methanol was added ketone **5** (1.5 g, 7.8 mmol). The colorless crystalline tosylhydrazone solid that formed slowly overnight was filtered and washed with 1:1 pentane/ether to yield **6** (1.9 g, 5.3 mmol, 68%), mp 153–154 °C, as a ca. 1:1 mixture of *E* and *Z* stereoisomers (with respect to the C=N bond). ¹H NMR (500 MHz, CDCl₃) δ 7.68 (dd, 2H), 7.15 (d, 2H), 2.55 (dt, 1H), 2.32 (br s, 1H); 2.29, 2.28 (2 s, 3H); 2.12 (m, 1H), 2.04 (m, 2H), 1.97 (m, 1H), 1.71 (m, 4H), 1.52 (m, 4H), 1.36 (m, 4H), 1.09 (m, 1H), 0.90 (m, 1H), 0.81 (q, 1H). ¹³C NMR (125 MHz, CDCl₃) δ 143.80, 143.77 (=C); 135.53, 135.45 (=C); 129.92, 128.26 (C=N); 129.46, 129.29 (2 =CH); 128.04, 127.94 (2 =CH); 42.71, 42.02, 41.67, 41.59, 41.54, 35.92, 35.74, 35.24 (CH); 33.34, 32.78, 32.75, 32.00, 31.96, 31.94, 31.86, 30.32, 29.30, 29.16, 28.36, 27.60, 27.40, 25.69 (CH₂); 21.59, 21.57 (CH₃); 20.71, 18.92 (CH₂). FTIR (neat) ν_{max} 3217, 2912, 1600, 1315, 1163 cm⁻¹. LRMS (EI) *m/z* 360 (M⁺, 1), 265 (21), 205 (53),

109 (99), 91 (74), 80 (100); HRMS (EI) calcd for $C_{20}H_{28}N_2O_2S$ 360.1872, found 360.1862.

cis,anti,cis-Tricyclo[7.4.0.0^{2,8}]tridec-10-ene (13TCT). Tosylhydrazone **6** (2.4 g, 6.7 mmol) was placed in a flame-dried apparatus, suspended in 15 mL of anhydrous TMEDA at rt, and then cooled to $-78\text{ }^\circ\text{C}$; CH_3Li (1.6 M in diethyl ether, 18.7 mL, 29.9 mmol) was added dropwise over 2.5 h. The reaction mixture was allowed to warm to rt and stirred overnight. Prior to workup the reaction mixture was cooled to $-30\text{ }^\circ\text{C}$ and quenched with 10 mL of cold water. The aqueous solution was extracted with pentane ($3 \times 150\text{ mL}$), and the combined organic extracts were washed with water, 1 N HCl, water, satd NaHCO_3 , water, and brine. The organic layer was dried (MgSO_4) and concentrated under reduced pressure to give **13TCT** as a colorless oil (0.66 g, 3.7 mmol, 56%). Further purification was achieved via preparative GC. ^1H NMR (500 MHz, CDCl_3) δ 5.82 (d, 1H), 5.73 (d, 1H), 2.17 (m, 3H), 2.02 (m, 3H), 1.80 (m, 5H), 1.61 (q, 1H), 1.52 (m, 2H), 1.38 (m, 1H), 1.23 (m, 1H), 1.06 (m, 2H). ^{13}C NMR (125 MHz, CDCl_3) δ 131.0 (=CH), 126.0 (=CH), 46.7 (CH), 38.9 (CH), 36.0 (CH), 35.5 (CH), 32.7 (CH_2), 32.5 (CH_2), 32.4 (CH_2), 30.1 (CH_2), 29.0 (CH_2), 23.6 (CH_2), 21.6 (CH_2). LRMS (m/z) 176 (M^+ , 3), 80 (100); HRMS (EI) calcd for $C_{13}H_{20}$ 176.1565, found 176.1572.

cis,anti,cis-Tricyclo[7.4.0.0^{2,8}]tridecane (7). A small sample of **13TCT** was subjected to a standard catalytic hydrogenation procedure^{5b} to give **7**, which was purified by preparative GC. ^1H NMR (500 MHz, CDCl_3) δ 2.09 (m, 2H), 1.88 (m, 2H), 1.79 (m, 2H), 1.74 (m, 3H), 1.64 (m, 2H), 1.43 (m, 3H), 1.36 (m, 3H), 1.25 (m, 3H), 1.06 (m, 2H). ^{13}C NMR (125 MHz, CDCl_3) δ 42.1 (2CH), 36.2 (2CH), 32.7 (CH_2), 32.1 (2 CH_2), 29.5 (2 CH_2), 28.0 (2 CH_2), 23.0 (2 CH_2). LRMS (m/z) 178 (M^+ , $C_{13}H_{22}$, 10), 96 (100), 81 (78), 67 (72).

trans-Tricyclo[7.2.2.0^{2,8}]tridec-10-ene (1) and endo-Tricyclo[7.2.2.0^{2,8}]trideca-2,10-diene (10). A sample of ketone mixture **8** and **9** was subjected to a three-step sequence^{5b} (standard LAH reduction, methanesulfonate formation, and standard LAH reduction) to give a mixture of **1** and **10** (19% and 81%, respectively, by GC analysis). Compound **1** (minor): ^{13}C NMR (125 MHz, CDCl_3) δ 136.1 (=CH), 131.6 (=CH), 44.0 (CH), 43.3 (CH), 36.7 (CH), 36.4 (CH), 34.5 (CH_2), 30.3 (CH_2), 29.3 (CH_2), 28.5 (CH_2), 28.1 (CH_2), 24.9 (CH_2), 18.0 (CH_2). LRMS (m/z) 176 (M^+ , $C_{13}H_{20}$, 26), 94 (25), 91 (36), 80 (100), 79 (48). Compound **10** (major): ^{13}C NMR (125 MHz, CDCl_3) δ 149.1 (=C), 132.5 (=CH), 132.3 (=CH), 120.3 (=CH), 47.2 (CH), 41.9 (CH), 39.3 (CH), 34.4 (CH_2), 32.5 (CH_2), 28.9 (CH_2), 27.5 (CH_2), 26.1 (CH_2), 25.4 (CH_2). LRMS (m/z) 174 (M^+ , $C_{13}H_{18}$, 47), 146 (100), 131 (44), 117 (66), 104 (61), 91 (44).

trans- and cis-Tricyclo[7.2.2.0^{2,8}]tridecane (11 and 12). A small sample of the mixture of compounds **1** and **10** was subjected to a standard catalytic hydrogenation procedure^{5b} to give a mixture of **11** and **12**. Compound **11** (major): ^{13}C NMR (125 MHz, CDCl_3) δ 42.4 (2CH), 33.3 (2 CH_2), 31.4 (2CH), 30.7 (CH_2), 28.9 (2 CH_2), 27.5 (2 CH_2), 21.0 (2 CH_2). LRMS (m/z) 178 (M^+ , $C_{13}H_{22}$, 100), 150 (22), 149 (22), 135 (54), 122 (25), 107 (20), 97 (49), 81 (64). Compound **12** (minor): ^{13}C NMR (125 MHz, CDCl_3) δ 42.2 (2CH), 32.2 (2CH), 32.0 (2 CH_2), 31.3 (CH_2), 27.1 (2 CH_2), 25.4 (2 CH_2), 20.8 (2 CH_2). LRMS (m/z) 178 (M^+ , $C_{13}H_{22}$, 100), 150 (26), 149 (21), 135 (62), 122 (43), 107 (20), 94 (34), 81 (52).

1,2-cis-2,8-trans-8,9-trans-Tricyclo[7.4.0.0^{2,8}]tridec-10-ene (13) and 1,2-trans-2,8-trans-8,9-cis-Tricyclo[7.4.0.0^{2,8}]tridec-10-ene (3). A less pure second crop of tosylhydrazone **6** (mp 149–151 $^\circ\text{C}$) was subjected to the Shapiro modification of the Bamford–Stevens reaction, as in the preparation of **13TCT**, to give a 4:1 mixture of **13TCT** and **13**, respectively. A more impure third crop of tosylhydrazone **6** (mp 138–146 $^\circ\text{C}$), upon similar treatment, gave a 7:2:1 mixture of **13TCT**:**13**:**3**, respectively. A fourth crop of impure tosylhydrazone **6** (mp 89–100 $^\circ\text{C}$), upon similar treatment, gave a mixture consisting of 27% **13TCT**, 33% **13**, and 40% **3** (by GC analysis). Compound **13**: ^{13}C NMR (125 MHz, CDCl_3) δ 129.8 (=CH), 127.8 (=CH), 48.2 (CH), 41.8 (CH), 38.6 (CH), 33.7 (CH), 33.6 (CH_2), 30.0 (CH_2), 29.0 (CH_2), 26.2 (CH_2), 26.1 (CH_2), 23.2

(CH_2), 22.3 (CH_2). LRMS (m/z) 176 (M^+ , $C_{13}H_{20}$, 7), 94 (12), 91 (10), 80 (100), 79 (41). Compound **3**: ^{13}C NMR (125 MHz, CDCl_3) δ 128.4 (=CH), 127.7 (=CH), 45.4 (CH), 40.4 (CH), 37.6 (CH), 33.6 (CH), 32.9 (CH_2), 29.8 (CH_2), 29.2 (CH_2), 27.6 (CH_2), 25.9 (CH_2), 21.7 (CH_2), 21.3 (CH_2). LRMS (m/z) 176 (M^+ , $C_{13}H_{20}$, 2), 91 (7), 80 (100), 79 (29).

cis,anti,cis-Tricyclo[7.4.0.0^{2,8}]tridecane (7) and trans,cis-Tricyclo[7.4.0.0^{2,8}]tridecane (14). The 4:1 mixture of **13TCT** and **13** prepared above was subjected to a standard catalytic hydrogenation procedure to yield a 4:1 mixture of **7** and **14**, respectively. Compound **14**: ^{13}C NMR (125 MHz, CDCl_3) δ 42.7 (CH), 40.7 (CH), 37.7 (CH), 34.0 (CH), 33.9 (CH_2), 30.3 (CH_2), 29.3 (CH_2), 26.6 (CH_2), 26.2 (CH_2), 25.5 (CH_2), 24.2 (CH_2), 23.8 (CH_2), 22.9 (CH_2). LRMS (m/z) 178 (M^+ , $C_{13}H_{22}$, 10), 97 (72), 96 (100), 81 (99), 67 (96).

■ ASSOCIATED CONTENT

● Supporting Information

Spectral characterization of **13TCT** and all products (or product mixtures); kinetic data and analysis. This material is available free of charge via the Internet at <http://pubs.acs.org>.

■ AUTHOR INFORMATION

Corresponding Author

*E-mail: phyllis.leber@fandm.edu.

Notes

The authors declare no competing financial interest.

■ ACKNOWLEDGMENTS

We acknowledge the Donors of the American Chemical Society Petroleum Research Fund and the Franklin & Marshall College Hackman Program for support of this research at Franklin & Marshall College.

■ REFERENCES

- (1) Woodward, R. B.; Hoffmann, R. *The Conservation of Orbital Symmetry*; Verlag Chemie: Weinheim, 1970.
- (2) Berson, J. A.; Dervan, P. B. *J. Am. Chem. Soc.* **1973**, *95*, 267–269; 269–270.
- (3) Leber, P. A.; Baldwin, J. E. *Acc. Chem. Res.* **2002**, *35*, 279–297.
- (4) (a) Bogle, X. S.; Leber, P. A.; McCullough, L. A.; Powers, D. C. *J. Org. Chem.* **2005**, *70*, 8913–8918. (b) Baldwin, J. E.; Leber, P. A.; Powers, D. C. *J. Am. Chem. Soc.* **2006**, *128*, 10020–10021. (c) Powers, D. C.; Leber, P. A.; Gallagher, S. S.; Higgs, A. T.; McCullough, L. A.; Baldwin, J. E. *J. Org. Chem.* **2007**, *72*, 187–194. (d) Leber, P. A.; Lasota, C. C.; Strotman, N. A.; Yen, G. S. *J. Org. Chem.* **2007**, *72*, 912–919.
- (5) (a) Baldwin, J. E.; Bogdan, A. R.; Leber, P. A.; Powers, D. C. *Org. Lett.* **2005**, *7*, 5195–5197. (b) Leber, P. A.; Bogdan, A. R.; Powers, D. C.; Baldwin, J. E. *Tetrahedron* **2007**, *63*, 6331–6338.
- (6) For structural data on cyclohexyl radicals, see: Bonazzola, L.; Leray, N.; Marx, R. *Chem. Phys. Lett.* **1974**, *24*, 88–90.
- (7) For structural data on cyclohexenyl radicals, see: (a) de Tannoux, N. M.; Pratt, D. W. *J. Chem. Soc., Chem. Commun.* **1978**, 394–395. (b) Hori, Y.; Shimada, S.; Kashiwabara, H. *J. Phys. Chem.* **1989**, *93*, 6007–6012.
- (8) For structural comparisons of cyclohexyl and cycloheptyl radicals, see: Burkey, T. J.; Griller, D.; Sutcliffe, R. *J. Org. Chem.* **1985**, *50*, 1138–1140. (b) Hori, Y.; Shimada, S.; Kashiwabara, H. *J. Phys. Chem.* **1986**, *90*, 3073–3079. (c) Liu, R.; Allinger, N. L. *J. Comput. Chem.* **1994**, *15*, 283–299.
- (9) Salomon, R. G.; Folting, K.; Streib, W. E.; Kochi, J. K. *J. Am. Chem. Soc.* **1974**, *96*, 1145–1152.
- (10) Fringuelli, F.; Guo, M.; Minuti, L.; Pizzo, F.; Tatichhi, A.; Wenkert, E. *J. Org. Chem.* **1989**, *54*, 710–712.
- (11) All GC analyses were acquired on an HP cross-linked methyl silicone column (50 m \times 0.2 mm i.d. \times 0.10 μm film thickness) using the temperature program: initial temperature of 110 $^\circ\text{C}$ for 1 min with

a temperature ramp of 0.1 °C/min. GC retention times (min) for all species in order of increasing elution time are as follows: **10** (23.8), **1** (25.2), **2** (25.9), **7** (26.2), **13TCT** (26.3), **3** (26.8), **14** (27.9), **13** (28.7), **11** (30.2), **12** (31.7).

(12) Northrop, B. H.; Houk, K. N. *J. Org. Chem.* **2006**, *71*, 3–13.

(13) (a) Carpenter, B. K. *J. Org. Chem.* **1992**, *57*, 4645–4648.

(b) Carpenter, B. K. *J. Am. Chem. Soc.* **1995**, *117*, 6336–6344.

(c) Carpenter, B. K. *Angew. Chem., Int. Ed.* **1998**, *37*, 3340–3350.

(14) Beno, B. R.; Wilsey, S.; Houk, K. N. *J. Am. Chem. Soc.* **1999**, *121*, 4816–4826.

(15) The close correspondence between calculated and experimental kinetic data, as seen in the Supporting Information materials, precludes reversion of product **3** to **13TCT**.

(16) Tao, H.-R.; Fang, D.-C. *Theor. Chem. Acc.* **2008**, *121*, 91–101.